PHYSICAL REVIEW A **92**, 040502(R) (2015)

# Electron dynamics following photoionization: Decoherence due to the nuclear-wave-packet width

Morgane Vacher,[1] Lee Steinberg,[2] Andrew J. Jenkins,[1] Michael J. Bearpark,[1] and Michael A. Robb[1,*]
[1]*Department of Chemistry, Imperial College London, London SW7 2AZ, United Kingdom*
[2]*School of Chemistry, University of Bristol, Bristol BS8 1TS, United Kingdom*
(Received 5 March 2015; published 20 October 2015)

The advent of attosecond techniques opens up the possibility to observe experimentally electron dynamics following ionization of molecules. Theoretical studies of pure electron dynamics at single fixed nuclear geometries in molecules have demonstrated oscillatory charge migration at a well-defined frequency but often neglecting the natural width of the nuclear wave packet. The effect on electron dynamics of the spatial delocalization of the nuclei is an outstanding question. Here, we show how the inherent distribution of nuclear geometries leads to dephasing. Using a simple analytical model, we demonstrate that the conditions for a long-lived electronic coherence are a narrow nuclear wave packet and almost parallel potential-energy surfaces of the states involved. We demonstrate with numerical simulations the decoherence of electron dynamics for two real molecular systems (paraxylene and polycyclic norbornadiene), which exhibit different decoherence time scales. To represent the quantum distribution of geometries of the nuclear wave packet, the Wigner distribution function is used. The electron dynamics decoherence result has significant implications for the interpretation of attosecond spectroscopy experiments since one no longer expects long-lived oscillations.

DOI: 10.1103/PhysRevA.92.040502 PACS number(s): 31.70.Hq, 33.80.Eh, 42.65.Re

The generation of attosecond pulses in the extreme ultraviolet range (using high harmonic generation in gases) [1,2] has opened up the possibility to probe dynamics in atoms, molecules, and solids with attosecond resolution [3–5]—the natural time scale of electronic motion. Attosecond techniques have since been developed and applied successfully to a range of problems, including the real-time observation of electronic relaxation in krypton atoms [6], the measurement of delays in photoemission of electrons in condensed-matter [7] and atomic [8] systems using the streaking technique, and the observation of electron dynamics in krypton atoms upon valence ionization using transient absorption spectroscopy [9].

One key target of attosecond experiments remains the real-time observation and control of electron dynamics upon ionization in molecules [10–17]. The interference between electronic eigenstates, populated coherently, alternates between constructive and destructive and leads to oscillating motion of the electronic density with a period inversely proportional to the energy gap. This is "pure" electron dynamics (i.e., takes place even if the nuclei are fixed) and is often called *charge migration* in the literature [18] or *hole migration* if it is induced by electron correlation [19,20].

A fascinating and outstanding question in the theoretical description of electron dynamics in molecules is the effect of the nuclei since most studies are carried out at a single fixed nuclear geometry (usually the equilibrium geometry of the neutral species) [21–26]. (Some studies include several conformers [22,27] but again with a single geometry per conformer.) These simulations predict long-lived oscillating motion in the electronic density at a well-defined frequency, but they neglect both the spatial delocalization of the nuclear wave packet and the nuclear motion. We have previously shown examples of how nuclear motion affects electron dynamics after a few femtoseconds [28–30]. Despré and coworkers recently simulated hole migration at a small number of distorted geometries [31]. Therefore, as yet, the effect of the width of the nuclear wave packet has not been extensively studied.

In the present Rapid Communication, we investigate the extent to which the single-geometry approximation is valid. By using the Wigner distribution function [32]—a quantum distribution function in classical phase space—to represent the delocalized nuclear wave packet, we propose a more realistic approach to describe electron dynamics in molecules. A distribution of fixed nuclear geometries leads to a distribution in initial energy gaps and therefore of oscillation periods in the electronic density (Fig. 1). We show that, as a result of the nuclear-wave-packet delocalization, it takes only a few femtoseconds for the electron dynamics to decohere for the two molecules studied. This calls into question the commonly held picture of long-lived electronic oscillations at a well-defined frequency.

In order to get some physical insight about the decoherence of electron dynamics due to the distribution of nuclear geometries, we first present a simple analytical model. Let us consider a system with one nuclear degree of freedom $R$ and three electronic states (Fig. 1): the ground state of the neutral species and the ground and first excited states of the cation. Using a linear approximation of the cation state energies, the energy gap between the cationic states reads as

$$\Delta E(R) = d|R|, \tag{1}$$

where the parameter $d$ is the difference in gradients of the two potential-energy curves. Note that Eq. (1) implies a point of degeneracy at $R = 0$ that does not need to exist (Fig. 1).

Before ionization, the neutral system is assumed to be in its electronic and vibrational ground states. In the harmonic approximation, the vibrational ground-state wave function is a normalized Gaussian,

$$g(R) = \left(\frac{2a}{\pi}\right)^{1/4} \exp[-a(R-b)^2]. \tag{2}$$

*mike.robb@imperial.ac.uk

 

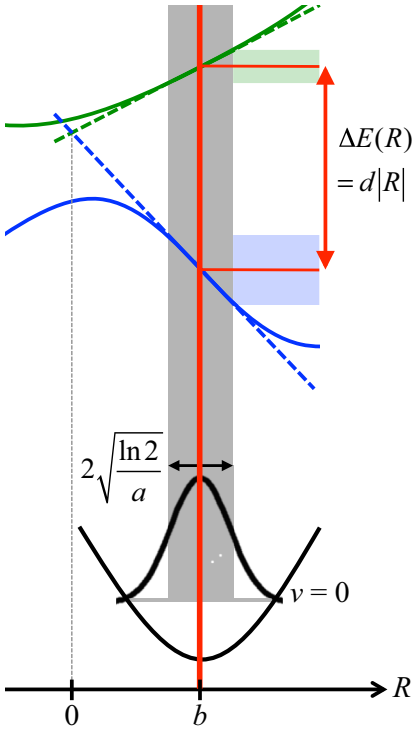


FIG. 1. (Color online) Ionization process in a model system. The lower curve represents the ground state of the neutral species; the upper two curves represent the ground and first excited states of the cation. The parameter $a$ determines the width of the Gaussian wave packet; $b$ determines the position of the equilibrium geometry of the neutral species with respect to the implied point of degeneracy in the cation; $d$ is the difference of gradients of the two cationic potential-energy curves.

The parameter $a$ determines the width of the Gaussian; $b$ determines the center, i.e., the position of the equilibrium geometry of the neutral species with respect to the implied point of degeneracy in the cation [Fig. 1 and Eq. (1)].

Let us consider a prompt ionization (by a pulse of broad bandwidth for instance) that leads to a coherent superposition of the two electronic states of the cation,

$$\Psi(\boldsymbol{r},R,t=0) = g(R)[c_0\psi_0(\boldsymbol{r};R) + c_1\psi_1(\boldsymbol{r};R)], \quad (3)$$

where the expansion coefficients in the adiabatic basis $c_0$ and $c_1$ are assumed to be independent of the geometry $R$ for simplicity. By solving the electronic time-dependent Schrödinger equation with fixed nuclei, one obtains the following time-dependent wave function (in atomic units):

$$\begin{aligned}\Psi(\boldsymbol{r},R,t) = g(R)\{&c_0\exp[-iE_0(R)t]\psi_0(\boldsymbol{r};R)\\ &+c_1\exp[-iE_1(R)t]\psi_1(\boldsymbol{r};R)\}. \quad (4)\end{aligned}$$

The electronic density is obtained by multiplying the wave function by its complex conjugate and integrating over all but one electronic spatial coordinate. Assuming real initial expansion coefficients and real basis states, it reads

$$\begin{aligned}\rho(r,R,t) = &|g(R)|^2[|c_0|^2\rho_{00}(r;R) + |c_1|^2\rho_{11}(r;R)]\\ &+2c_0c_1|g(R)|^2\cos[\Delta E(R)t]\rho_{01}(r;R), \quad (5)\end{aligned}$$

with $\rho_{ij}(r;R) = \int dr^{N-1}\psi_i(\boldsymbol{r};R)\psi_j(\boldsymbol{r};R)$. Note that the last term of Eq. (5), noted as $C(r,R,t)$ hereafter, is the sum of the off-diagonal elements of the electronic density matrix that are also called *electronic coherences*. It corresponds to the interference between the two electronic states, alternating between constructive and destructive, with a period inversely proportional to the energy gap between the two eigenstates—and therefore $R$ dependent,

$$T(R) = \frac{2\pi}{\Delta E(R)}. \quad (6)$$

The amplitude of the oscillations depends on the product of expansion coefficients $c_0c_1$.

The effect of the spatial delocalization of the nuclei is taken into account by calculating the expectation value over the range of nuclear geometries,

$$\langle C(r,t)\rangle = 2c_0c_1\int dR|g(R)|^2\cos[\Delta E(R)t]\rho_{01}(r;R), \quad (7)$$

where $|g(R)|^2$ is the probability density function. If $\rho_{01}(r;R)$ does not change much with $R$, it can be approximated to the constant $\rho_{01}(r;b)$. Equation (7) then reads

$$\langle C(r,t)\rangle \approx 2c_0c_1\cos(dbt)\exp(-d^2t^2/8a)\rho_{01}(r;b). \quad (8)$$

We get back the cosine oscillation of the equilibrium geometry $R=b$ but diminished with time by a Gaussian function. As $t\to\infty$, the electronic coherences disappear: $\langle C(r,t)\rangle \to 0$. The system *decoheres*. Note that here the origin of the decoherence is not the coupling with an environment but rather the *dephasing* of the different oscillations. One can define a coherence half-life as the time at which the amplitude of the cosine oscillation is reduced to half its initial value due to the Gaussian decay,

$$t_{1/2} = \frac{2\sqrt{2\ln 2a}}{d}. \quad (9)$$

The coherence half-life depends on the physical properties of the system. It is long if: (i) The wave packet is narrow (large $a$), or (ii) the two potential-energy curves are almost parallel (small $d$). Indeed, both characteristics result in a narrow energy-gap distribution which postpones the dephasing. The position of the equilibrium geometry of the neutral species $b$ does not affect $t_{1/2}$; it only determines the period of oscillations.

Our simple analytical model shows how the nuclear-wave-packet width leads to the dephasing of the electron dynamics oscillations. It also provides the general conditions for long-lived electron dynamics. Note that it has several limitations: The nuclei are kept fixed (the kinetic operator of the nuclei is absent from the Hamiltonian of the system), and the interaction between the cation and the photoelectron is not taken into account (assuming a photoelectron with high kinetic energy and therefore ionization by a high-energy photon). Also, the electronic density is calculated as an expectation value over all nuclear geometries treated independently.

Let us now move beyond the model system treated above and investigate numerically the decoherence of electron dynamics in two real molecular systems: paraxylene and polycyclic norbornadiene (PLN) cations (Fig. 2). In both

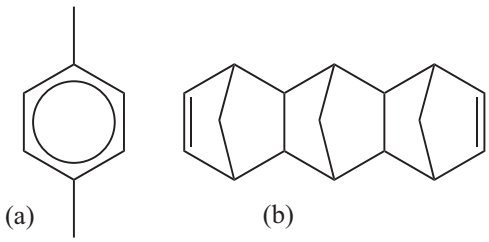


FIG. 2. Structures of (a) paraxylene and (b) PLN.

molecules, the equilibrium geometry of the neutral species is in the vicinity of a crossing between the two lowest-energy electronic states of the cationic species [30,33–35]. The nonzero energy gap at the equilibrium geometry of the neutral species is needed to induce the electron dynamics we study.

In both molecules, the two cationic states correspond to ionization of the $\pi$ system. These two states are relatively close in energy and well separated from higher excited states [30,36]. Therefore, the generation by photoionization of a coherent superposition of only these two states by, for instance, a short pulse of broad bandwidth is reasonable. The exact composition of the superposition—relative weight and phase—will depend on any experimental setup. Here a 50:50 and a 60:40 in-phase superposition of cationic states will be considered in paraxylene in order to represent a range of possible superpositions generated by experiment. By doing that, we test the sensitivity of the results with respect to the initial conditions.

In practice, time is discretized, and the electronic wave function is propagated by numerically solving the time-dependent Schrödinger equation, assuming a constant Hamiltonian over the time step [37,38]. We use a time step of 0.05 fs and state-averaged complete active space self-consistent field (CASSCF) electronic basis states to expand the electronic wave function. Using the standard 6-31G* basis set, we choose the $\pi$ orbitals as active: six orbitals in paraxylene and four in PLN.

To follow the evolution of the electronic wave function, its electronic spin density—that allows one to locate the unpaired electron—is computed at each step of the simulation [30,37]. Because of two resonance structures where the unpaired electron and the positive charge are interchanged, locating the unpaired electron is equivalent to locating the positive charge. This is how we monitor the hole dynamics. Note that similar to the hole density of Ref. [20], the electronic spin density is a theoretical tool to follow the electron dynamics; yet, the conclusions we draw from it will apply to any observable related to the electronic density.

We have first simulated electron dynamics at the equilibrium geometries of the neutral species [optimized at the CASSCF(6,6)/6-31G* level of theory for paraxylene and B3LYP/6-31G* for PLN]. In Fig. 3, there are snapshots of the spin densities as a function of time during the first half oscillation. In paraxylene, the spin density swings from one side of the phenyl ring to the other in approximately $T/2 = 5.2$ fs; in PLN, the spin density initially localized on the right double bond migrates to the left one in approximately $T/2 = 7.6$ fs. Such spin densities can be used as points along a "scale of electron dynamics": We chose the state $\frac{1}{\sqrt{2}}(\psi_0 + \psi_1)$ to define the spin density $+1$, $\frac{1}{\sqrt{2}}(\psi_0 + i\psi_1)$ to define the spin density 0, and $\frac{1}{\sqrt{2}}(\psi_0 - \psi_1)$ to define the spin density $-1$.

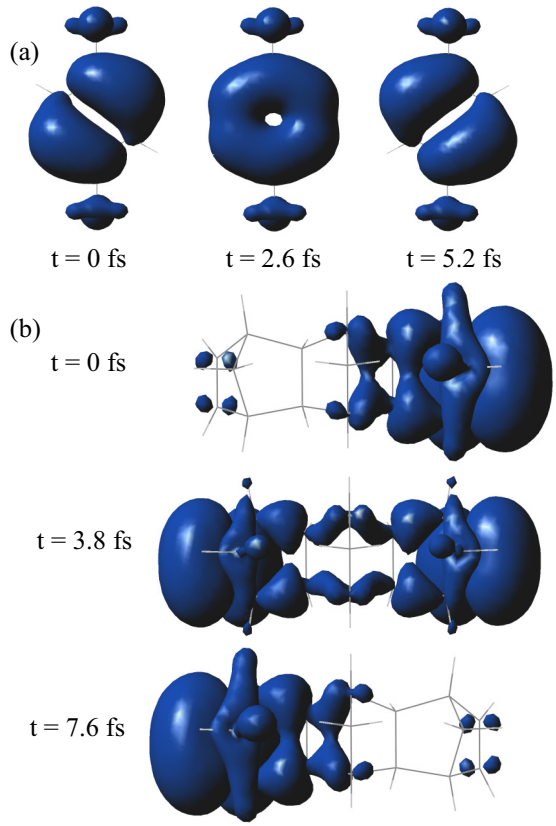


FIG. 3. (Color online) Snapshots of the electronic spin densities after ionization of the $\pi$ system in (a) paraxylene and (b) PLN at $t = 0$, $t = \frac{T}{4}$, and $t = \frac{T}{2}$.

The electron dynamics is represented along that scale as a function of time in Fig. 4: We see perfect sinusoidal oscillations. The larger energy gap in the paraxylene cation compared to the one in the PLN cation explains the faster electron dynamics [Table I and Eq. (6)]. Using a nonequally weighted superposition (dashed curve) does not affect the period of oscillations but decreases the amplitude of the oscillations as expected.

We have also simulated in the paraxylene cation electron dynamics with the nuclei allowed to move according to the Ehrenfest method [37–39]. The spin-density oscillation with nuclei moving (solid thin curve) is identical to the one with fixed nuclei (solid thick curve) up to 4 fs; then, the oscillation speeds up [30]. The key point is that, in the paraxylene cation,

TABLE I. Energy gap at the equilibrium geometry and averaged energy gap (standard deviation) for the distribution of geometries, calculated at the CASSCF/6-31G* level.

| Molecule | Energy gap at equilibrium (eV) | Averaged energy gap (standard deviation) (eV) |
|---|---|---|
| Paraxylene | 0.39 | 0.51 (0.25) |
| PLN | 0.27 | 0.36 (0.12) |

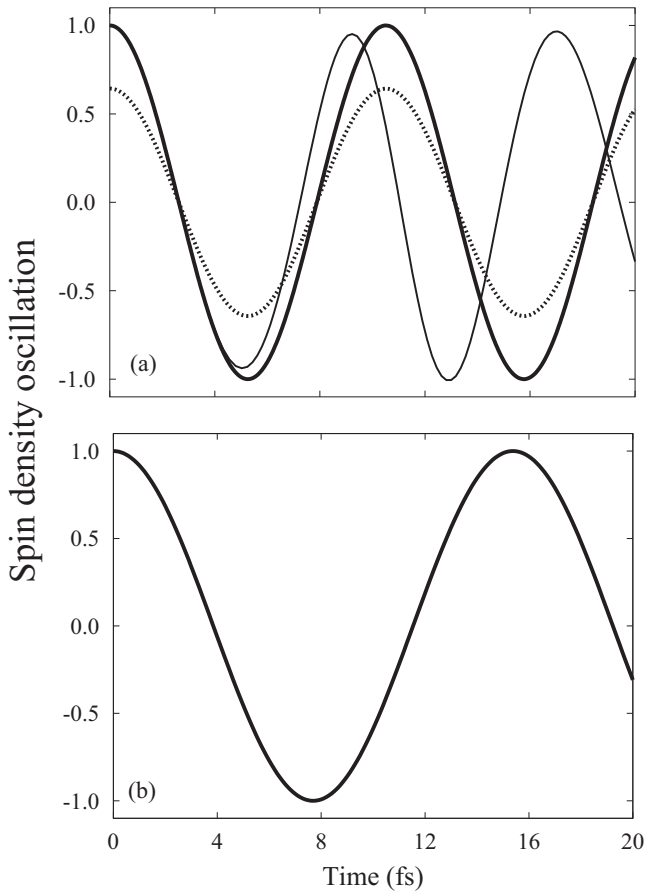


FIG. 4. Electron dynamics following ionization of the $\pi$ system of (a) paraxylene and (b) PLN. The simulation is initiated at the equilibrium geometry of the neutral species with fixed nuclei (thick curve) or nuclei moving (thin curve). The initial electronic wave function is a 50:50 (solid curve) or 60:40 (dashed curve) superposition of $\psi_0$ and $\psi_1$.

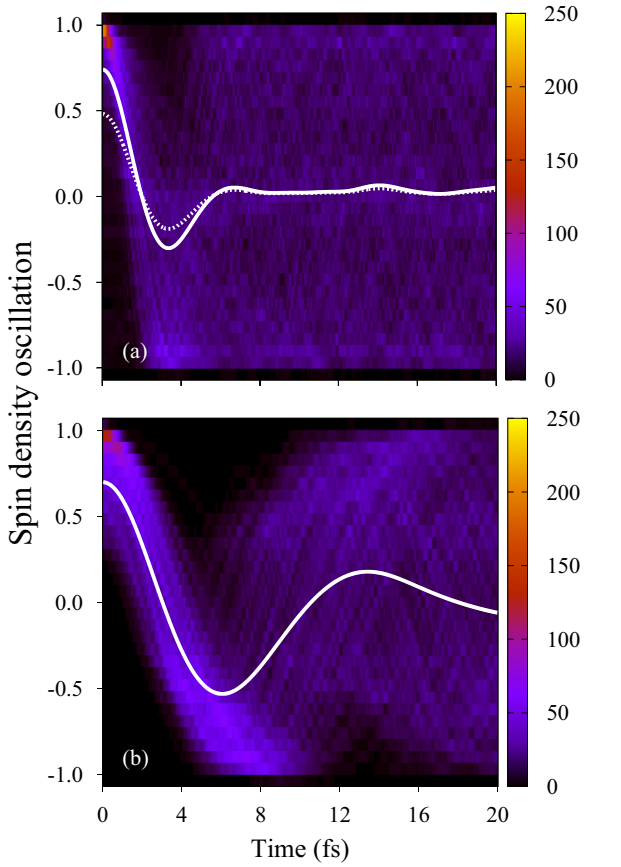


FIG. 5. (Color online) Electron dynamics in (a) paraxylene and (b) PLN as in Fig. 4 for the ensemble of nuclear geometries. The nuclear distribution (500 sampled geometries) reproduces the vibrational ground state before ionization. The white lines represent the averaged electron dynamics for the 50:50 (solid lines) and 60:40 (dashed lines) superpositions of $\psi_0$ and $\psi_1$.

the electron dynamics is modified but not destroyed by the nuclear motion within the Ehrenfest approximation.

To assess the validity of the single-geometry approximation, these oscillations must be compared to those in the case of an ensemble of fixed geometries (distributed around the equilibrium geometries). For each system, 500 nuclear geometries were sampled from the Wigner distribution functions using the NEWTON-X package [40]. Use of the Wigner distribution enables us to mimic the quantum distributions of the vibrational ground states (in the harmonic approximation). As the results depend on the number of sampled geometries considered, one must make sure convergence has been reached. The resulting averaged energy gaps and standard deviations are indicated in Table I. Note that the averaged energy gap is not equal to the energy gap at the equilibrium geometry because of the asymmetry of the cationic potential-energy surfaces.

In the paraxylene cation, Fig. 5(a) shows the electron dynamics—as in Fig. 4(a)—for the ensemble of nuclear geometries, simulated independently. A close look allows one to distinguish the individual oscillations (with different periods) that dephase with time. The average oscillation amplitudes are shown as white lines. We see a half oscillation reaching its turning point at about 3 fs, and then it goes to zero: The coherent electron dynamics quickly disappears. By fitting the averaged oscillation amplitude to Eq. (8) over the first 10 fs, a coherence half-life is extracted: $t_{1/2} \approx 4$ fs. The dephasing is so fast that there is not even a single oscillation in the electronic spin density. Note that the same conclusion holds with a nonequally weighted superposition (dashed line), showing the robustness of these results with respect to the initial conditions.

In PLN, the energy-gap distribution is about twice as narrow as in paraxylene (Table I). This is partly due to the topology of the cationic potential-energy surfaces (parameter $d$ in our model system). In paraxylene, the equilibrium geometry of the neutral species is in the vicinity of a peaked conical intersection in the cation [30]: The difference in gradients $d$ is thus rather large. In PLN, the neutral geometry corresponds to an avoided crossing in the cation [34]: On both surfaces, the gradient is small leading to a small difference in gradients $d$. As a result, the oscillation in the spin density survives longer despite their damped amplitudes [Fig. 5(b)]. A coherence half-life of $t_{1/2} \approx 10$ fs was extracted.

We conclude that the simple picture of long-lived electron dynamics at a well-defined frequency predicted by the single-geometry approximation cannot survive the natural width of the nuclear wave packet. Using a combination of an analytical

model and numerical simulations of electron dynamics in real molecules, we show that electronic oscillations will dephase due to the spatial delocalization of the nuclei. Our simple analytical model provides the general conditions for long-lived electron dynamics and enables the definition of molecular targets in which this can be observed. With our method of using a Wigner distribution of geometries to represent the nuclear wave packet, we give a more realistic description of electron dynamics that goes far beyond what has been done before.

The decoherence effect of electron dynamics is general and will be common to all molecular systems. We demonstrate the role of the topology of the potential-energy surfaces in the time scale of decoherence with the two molecules studied here exhibiting different coherence half-lives. A key result is that the effect on electron dynamics of the nuclear-wave-packet width can be larger than the effect of the nuclear motion as shown here in paraxylene (within the Ehrenfest approximation).

Our results will have significant implications for the interpretation of attosecond spectroscopy experiments since one no longer *expects* long-lived oscillations. At present, most experiments that aimed at observing ultrafast dynamics have used a strong infrared field [3,15]; this may actually perturb and be driving the observed dynamics rather than allowing an observation of the dynamics intrinsic to the molecule (a complication that has motivated the development of the attosecond pump—attosecond probe experiments [41]). Several measurements have already been suggested to observe electron dynamics: time-resolved Auger spectra [42], photoelectron angular distributions [43], or x-ray absorption spectra [44,45]—the electronic transition probability being proportional to the time-dependent electronic density in each case. Such experiments would allow the observation of the decoherence of electron dynamics that we predict.

This work was supported by UK-EPSRC Grant No. EP/I032517/1. All calculations were run using the Imperial College High Performance Computing service. The authors thank C. Fare, J. Malhado, F. McGrath, P. G. Hawkins, V. Averbukh, and J. P. Marangos for helpful discussions.

[1] M. Hentschel, R. Kienberger, C. Spielmann, G. A. Reider, N. Milosevic, T. Brabec, P. Corkum, U. Heinzmann, M. Drescher, and F. Krausz, Nature (London) **414**, 509 (2001).

[2] P. M. Paul, E. S. Toma, P. Breger, G. Mullot, F. Augé, P. Balcou, H. G. Muller, and P. Agostini, Science **292**, 1689 (2001).

[3] S. Baker, J. S. Robinson, C. A. Haworth, H. Teng, R. A. Smith, C. C. Chirilă, M. Lein, J. W. G. Tisch, and J. P. Marangos, Science **312**, 424 (2006).

[4] M. Lein, Phys. Rev. Lett. **94**, 053004 (2005).

[5] S. Patchkovskii, Phys. Rev. Lett. **102**, 253602 (2009).

[6] M. Drescher, M. Hentschel, R. Kienberger, M. Uiberacker, V. Yakovlev, A. Scrinzi, T. Westerwalbesloh, U. Kleineberg, U. Heinzmann, and F. Krausz, Nature (London) **419**, 803 (2002).

[7] A. L. Cavalieri, N. Müller, T. Uphues, V. Yakovlev, A. Baltuska, B. Horvath, B. Schmidt, L. Blümel, R. Holzwarth, S. Hendel, M. Drescher, U. Kleineberg, P. Echenique, R. Kienberger, F. Krausz *et al.*, Nature (London) **449**, 1029 (2007).

[8] M. Schultze, M. Fieß, N. Karpowicz, J. Gagnon, M. Korbman, M. Hofstetter, S. Neppl, A. Cavalieri, Y. Komninos, T. Mercouris, C. Nicolaides, R. Pazourek, S. Nagele, J. Feist, J. Burgdörfer *et al.*, Science **328**, 1658 (2010).

[9] E. Goulielmakis, Z.-H. Loh, A. Wirth, R. Santra, N. Rohringer, V. S. Yakovlev, S. Zherebtsov, T. Pfeifer, A. M. Azzeer, M. F. Kling, S. R. Leone, and F. Krausz, Nature (London) **466**, 739 (2010).

[10] M. F. Kling and M. J. J. Vrakking, Annu. Rev. Phys. Chem. **59**, 463 (2008).

[11] F. Krausz and M. Y. Ivanov, Rev. Mod. Phys. **81**, 163 (2009).

[12] A. I. Kuleff and L. S. Cederbaum, Phys. Rev. Lett. **106**, 053001 (2011).

[13] L. Belshaw, F. Calegari, M. J. Duffy, A. Trabattoni, L. Poletto, M. Nisoli, and J. B. Greenwood, J. Phys. Chem. Lett. **3**, 3751 (2012).

[14] J. Leeuwenburgh, B. Cooper, V. Averbukh, J. P. Marangos, and M. Y. Ivanov, Phys. Rev. Lett. **111**, 123002 (2013).

[15] F. Calegari, D. Ayuso, A. Trabattoni, L. Belshaw, S. De Camillis, S. Anumula, F. Frassetto, L. Poletto, A. Palacios, P. Decleva, J. B. Greenwood, F. Martín, and M. Nisoli, Science **346**, 336 (2014).

[16] S. R. Leone, C. W. McCurdy, J. Burgdorfer, L. S. Cederbaum, Z. Chang, N. Dudovich, J. Feist, C. H. Greene, M. Ivanov, R. Kienberger, U. Keller, M. F. Kling, Z.-H. Loh, T. Pfeifer, A. N. Pfeiffer *et al.*, Nat. Photon. **8**, 162 (2014).

[17] F. Lepine, M. Y. Ivanov, and M. J. J. Vrakking, Nat. Photon. **8**, 195 (2014).

[18] A. I. Kuleff and L. S. Cederbaum, J. Phys. B: At. Mol. Opt. Phys. **47**, 124002 (2014).

[19] L. S. Cederbaum and J. Zobeley, Chem. Phys. Lett. **307**, 205 (1999).

[20] J. Breidbach and L. S. Cederbaum, J. Chem. Phys. **118**, 3983 (2003).

[21] F. Remacle and R. D. Levine, Z. Phys. Chem. **221**, 647 (2007).

[22] A. I. Kuleff and L. S. Cederbaum, Chem. Phys. **338**, 320 (2007).

[23] S. Lünnemann, A. I. Kuleff, and L. S. Cederbaum, Chem. Phys. Lett. **450**, 232 (2008).

[24] S. Lünnemann, A. I. Kuleff, and L. S. Cederbaum, J. Chem. Phys. **129**, 104305 (2008).

[25] G. Periyasamy, R. D. Levine, and F. Remacle, Chem. Phys. **366**, 129 (2009).

[26] A. I. Kuleff, S. Lünnemann, and L. S. Cederbaum, J. Phys. Chem. A **114**, 8676 (2010).

[27] B. Cooper, P. Kolorenc, L. J. Frasinski, V. Averbukh, and J. P. Marangos, Faraday Discuss. **171**, 93 (2014).

[28] D. Mendive-Tapia, M. Vacher, M. J. Bearpark, and M. A. Robb, J. Chem. Phys. **139**, 044110 (2013).

[29] M. Vacher, M. J. Bearpark, and M. A. Robb, J. Chem. Phys. **140**, 201102 (2014).

[30] M. Vacher, D. Mendive-Tapia, M. J. Bearpark, and M. A. Robb, J. Chem. Phys. **142**, 094105 (2015).

[31] V. Despré, A. Marciniak, V. Loriot, M. C. E. Galbraith, A. Rouzée, M. J. J. Vrakking, F. Lépine, and A. I. Kuleff, J. Phys. Chem. Lett. **6**, 426 (2015).
[32] E. Wigner, Phys. Rev. **40**, 749 (1932).
[33] M. J. Paterson, M. J. Bearpark, M. A. Robb, L. Blancafort, and G. A. Worth, Phys. Chem. Chem. Phys. **7**, 2100 (2005).
[34] L. Blancafort, F. Jolibois, M. Olivucci, and M. A. Robb, J. Am. Chem. Soc. **123**, 722 (2001).
[35] G. A. Jones, B. K. Carpenter, and M. N. Paddon-Row, J. Am. Chem. Soc. **120**, 5499 (1998).
[36] F. S. Jorgensen, M. N. Paddon-Row, and H. K. Patney, J. Chem. Soc., Chem. Commun., 573 (1983).
[37] M. Vacher, D. Mendive-Tapia, M. J. Bearpark, and M. A. Robb, Theor. Chem. Acc. **133**, 1505 (2014).
[38] M. J. Frisch, G. W. Trucks, H. B. Schlegel, G. E. Scuseria, M. A. Robb, J. R. Cheeseman, G. Scalmani, V. Barone, B. Mennucci, G. A. Petersson, H. Nakatsuji, M. Caricato, X. Li, H. P. Hratchian, A. F. Izmaylov *et al.*, Gaussian development version, revision h.32 (Gaussian, Inc., Wallingford, CT, 2010).
[39] P. Ehrenfest, Z. Phys. **45**, 455 (1927).
[40] M. Barbatti, G. Granucci, H. Lischka, M. Persico, and M. Ruckenbauer, NEWTON-X A package for Newtonian dynamics close to the crossing seam, version 0.11b, www.univie.ac.at/newtonx (2006).
[41] D. Fabris, T. Witting, W. A. Okell, D. J. Walke, P. Matia-Hernando, J. Henkel, T. R. Barillot, M. Lein, J. P. Marangos, and J. W. G. Tisch, Nat. Photon. **9**, 383 (2015).
[42] B. Cooper and V. Averbukh, Phys. Rev. Lett. **111**, 083004 (2013).
[43] B. Mignolet, R. D. Levine, and F. Remacle, J. Phys. B: At. Mol. Opt. Phys. **47**, 124011 (2014).
[44] A. D. Dutoi, K. Gokhberg, and L. S. Cederbaum, Phys. Rev. A **88**, 013419 (2013).
[45] A. D. Dutoi and L. S. Cederbaum, Phys. Rev. A **90**, 023414 (2014).